VISUAL SERVOING OF A MULTI-ROBOTIC SYSTEM FOR MANIPULATION TASKS

J. Pomares, F. A. Candelas, C. Jara, G. J. García, I. Perea and F. Torres
Physics, Systems Engineering and Signal Theory Department, University of Alicante, Alicante, Spain

Keywords: Multi-robotic system, Visual control, Modelling and control.

Abstract: This paper describes the visual servo control of a multi-robot system composed of a Mitsubishi PA10 robot (main robot) and a 3 degrees of freedom (DOF) mini-robot coupled to the main robot. The visual system composed of a single camera is located at the end-effector of the mini-robot. The acquired images are employed to guide the mini-robot in order to improve the scene visibility. Furthermore, these images are also used to guide the main robot. The paper also describes the main issues about the modelling and construction of the mini-robot.

1 INTRODUCTION

Visual servoing systems permit to carry out point-to-point motion of a robot using visual information. The most known classification for this kind of systems divides them in position-based and image-based visual servoing systems (Chaumette and Hutchinson, 2006). The first ones use 3D information of the real workspace to guide the robot and the second ones employ 2D information provided by the image camera. This last approximation is the used in this paper.

When a visually guided robot performs a manipulation task, the image features can be occluded by the robot tool, or by the own object geometry. These occlusions can appear not only in an eye-in-hand configuration (the camera is located at the end-effector of the robot), but also in an eye-to-hand approach (the camera observes the end-effector and the object). The problem of occlusions is an important topic of research in visual servoing systems. Using more than one camera can decrease the possibility of an occlusion event during the visual servoing task (Lippiello et al. 2007). The method proposed in (Iwatani et al. 2008) chooses a set of correctly extracted image features, and it then obtains an estimation of all the image features from the correctly extracted image features. In (Muis and Ohnishi, 2005) the problem is tackled introducing a second camera in order to have the benefits of both configurations: eye-in-hand and eye-to-hand. The eye-to-hand camera is located on a mobile robot that observes the manipulator (which mounts an eye-in-hand configuration). The same strategy is employed in (Flandin et al. 2000), where both camera configurations are fused to improve the visual servoing task.

In order to improve manipulation tasks while guiding the robot manipulator using a visual servoing scheme, a similar approach to (Muis and Ohnishi, 2005; Flandin et al. 2000) is proposed in this paper. However, in this paper a unique camera is employed to improve the scene visibility. The camera is located at the end-effector of a 3 DOF mini-robot. The images acquired from this camera permit the visual servo of this mini-robot. This mini-robot is located at the end-effector of a 7 DOF manipulator (main robot). This main robot is also guided using the images obtained from the camera positioned at the mini-robot. To do so, a virtual camera located at the main robot end-effector is employed. Thus, the real camera is positioned in the scene by the mini-robot increasing the manipulation task visibility, whereas the virtual camera guides the main robot to accomplish the manipulation task. This is the main approach described in the paper.

This paper is organized as follows: Section II describes the design of the mini-robot. In Section III, the visual-servo control of the multi-robot system is described. Section IV shows experimental results obtained. Finally, some conclusions are discussed in Section V.

Pomares J., Candelas F., Jara C., García G., Perea I. and Torres F..
VISUAL SERVOING OF A MULTI-ROBOTIC SYSTEM FOR MANIPULATION TASKS.
DOI: 10.5220/0003521301610166
In *Proceedings of the 8th International Conference on Informatics in Control, Automation and Robotics* (ICINCO-2011), pages 161-166
ISBN: 978-989-8425-75-1

2 DESIGN OF THE MINI-ROBOT

2.1 Geometric Description

The mini-robot is attached at the end of the robotic manipulator PA-10 with the aim of obtaining a suitable viewing point for handling tasks correctly (see Figure 1). In order to solve this problem, a joint RRR robot with three rotational DOF has been developed. This mini-robot will obtain the optimal viewpoint around the manipulation task performed by the main robot. All the rotary joints are independent of the main robot movement.

2.2 Main Mechanical Properties

The 3D modelling and simulation has been performed using the Virtual LAB software, which has permitted the components' design and dynamic simulation. This model has been made taking into account the maximum strength, lightness and adaptability.

The mini-robot requires a robust design since possible joint looseness can introduce errors in the model and this issue would complicate the subsequent control of the robotic system. The lightness of the robot is another important feature, because the Mitsubishi PA-10 robot is only able to handle 10 kg, and therefore the mini-robot must try to minimize the additional weight added to maintain adequate handling capacity. Another desired feature is to build a design to adapt the robot at the PA-10 without physical modifications in the latter.

Metallic pieces have been done using Duraluminium, a material that provides good resistance and low weight characteristics. The first joint turns on a bearing which has been designed with an interior space that permits to attach any tool

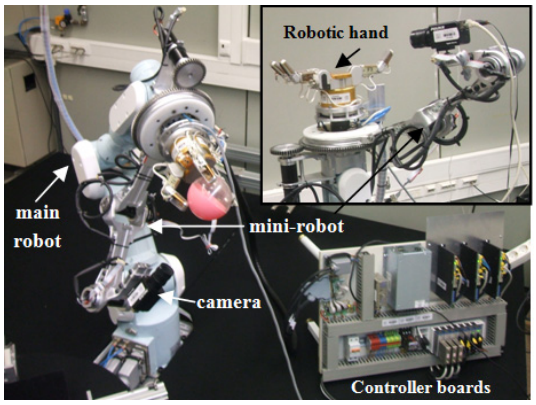

Figure 1: Mini-robot attached at the end of the main robot during a manipulation task.

at Mitsubishi PA-10 for manipulation tasks. This bearing is the rotation support part of the first joint, which has been constructed using a plastic material called PEUHMW. This material has high resistance to breakage and mechanical wear, a low density and low coefficient of friction to enable the rotation. Similar materials haven been employed for the second and third joints. The weight of the mini-robot built is approximately 5.5 kg.

3 VISUAL SERVO CONTROL OF THE ROBOTIC SYSTEM

3.1 Image-based Control

In image-based visual servoing systems, the controller input is a comparison between the observed image features, $\mathbf{s}$, and the desired ones, $\mathbf{s}^*$. This last set of features is observed by the eye-in-hand camera from the desired location. The vision system is located at the feedback of the control loop, and deals with the extraction of these features, $\mathbf{s}$, during the task (see Figure 2). The controller, comparing the real features and the desired ones, executes the necessary control actions in order to achieve the position where $\mathbf{s} = \mathbf{s}^*$. This technique is usually implemented in an external loop that provides an input to the robot internal controller. This approach corresponds with the indirect visual servoing and will be used in this paper to guide the mini-robot and the main robot. These approaches consider that the desired visual features $\mathbf{s}^*$ are learned.

A visual servoing task can be described by an m-dimensional image function, $\mathbf{e}_t$, which must be regulated to 0:

$$\mathbf{e}_t = \mathbf{C}\left(\mathbf{s} - \mathbf{s}^*\right) \quad (1)$$

where $\mathbf{s} = (f_1, f_2, \ldots f_k)$ is a kx1 vector containing k visual features observed at the current state ($f_i = (f_{ix}, f_{iy})$), while $\mathbf{s}^* = (f_1^*, f_2^*, \ldots f_k^*)$ denotes the desired features (extracted at the desired location). The visual features depends on the robot pose, $\mathbf{s} = \mathbf{s}(\mathbf{r}(t))$, where $\mathbf{r}(t)$ is the relative pose between the camera and the environment at time t. $\mathbf{C}$ is a m x k combination matrix that must be of full rank $m \leq k$ in order to produce the m independent components of $\mathbf{e}_t$.

In order to determine the value of the image-based controller, the concept of interaction matrix must be defined. This matrix, $\mathbf{L}_s$, relates the

variations in the image with the variations in the camera pose $\dot{\mathbf{s}} = \mathbf{L}_s \cdot \dot{\mathbf{r}}$ (Chaumette and Hutchinson, 2006). If, Rank($\mathbf{L}_s$) = m = k, $\mathbf{C} = \mathbf{I}_m$ and the following image-based controller is used:

$$\mathbf{v}^C = -\lambda \mathbf{L}_s^+ \left(\mathbf{s} - \mathbf{s}^*\right) \quad (2)$$

where $\mathbf{L}_s^+$ is the pseudo inverse of the interaction matrix. $\mathbf{L}_s^+$ is chosen as the Moore-Penrose pseudoinverse of $\mathbf{L}_s^+$, $\mathbf{L}_s^+ = \left(\mathbf{L}_s^T \mathbf{L}_s\right)^{-1} \mathbf{L}_s^T$.

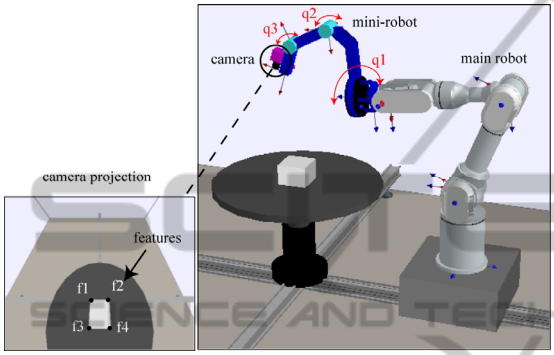

Figure 2: Image features extracted by the mini-robot.

3.2 Positioning of the Main Robot from the Visual Features Detected by the Mini-robot

In the previous paragraphs, the main properties of the employed image-based controller are described. However, in order to guide the main robot, some modifications must be performed in the previous approach. The controller described in Section 3.1 considers that an eye-in-hand camera is employed. However, in our case the camera is located at the end of the mini-robot. To overcome this problem, a Reference Virtual Camera (RVC) located at the end of the main robot is employed. The RVC is a virtual camera which will be employed to simulate the use of an eye-in-hand camera at the main robot.

In order to guide the mini-robot, the approach described in (Pomares et al. 2010) is employed. This approach allows the tracking of a given trajectory by using visual information. This trajectory is previously generated in order to guarantee that occlusions do not appear during the task. The tracking of this trajectory is performed using an image-based control with a non-time dependent behaviour.

As commented before, the visual information extracted by the camera located at the end of the mini-robot must be also used to guide the main robot. In this case, the image-based controller is:

$$\mathbf{v}^C = -\lambda \mathbf{L}_s^+ \left(\mathbf{s}_u - \mathbf{s}_u^*\right) \quad (3)$$

where $\mathbf{s}_u$ and $\mathbf{s}_u^*$ are the extracted and desired visual features considered by the RVC. In order to obtain these features, the approach described in the following paragraphs is employed.

First, we consider $\mathbf{M}_O^C$ as extrinsic parameters of the real camera located at the end of the mini-robot (pose of the observed object frame with respect to the camera frame, the super index indicates the coordinate frame with respect the referenced point). Therefore, an object 3D point, $\mathbf{P}_P^O$, can be expressed in the camera coordinate frame as:

$$\mathbf{P}_P^C \left(x_P^C, y_P^C, z_P^C\right) = \mathbf{M}_O^C \mathbf{P}_P^O \quad (4)$$

Considering a pin-hole camera projection model, the point $\mathbf{P}_P^C$ with 3D coordinates relative to the camera reference frame is projected onto the image plane at the 2D point $\mathbf{p}$. This point is computed from the camera focal length, f, as:

$$\mathbf{p} = (x, y)^T = \left(f \frac{x_P^C}{z_P^C}, f \frac{y_P^C}{z_P^C}\right)^T \quad (5)$$

Finally, the units of (5) specified in terms of metric units are scaled and transformed in pixels coordinates relative to the image reference frame, as:

$$\mathbf{s} = \left(f_x, f_y\right) = \left(u_0 + f_u x, v_0 + f_v y\right) \quad (6)$$

where (f_u, f_v, u_0, v_0) are the camera intrinsic parameters, The intrinsic parameters considered are the position of the optical center (u_0, v_0) and the size of the pixel and the focal length defined by (f_u, f_v).

In order to perform the main robot guidance using the RVC, the following steps have been implemented:

1. Considering $\mathbf{s}_m$ as the extracted visual features by the mini-robot, the pose of the observed object frame with respect the mini-robot camera $\mathbf{M}_O^{MC}$ must be obtained (estimation of the camera extrinsic parameters). To do that, the error indicated in Equation (7) is progressively cancelled. This error represents the difference between the observed data, $\mathbf{s}_m$, and the position of the same features computed by back-projection employing the current extrinsic parameters, $\mathbf{s}_p$ (to perform this projection, the Equations (4)-(6) are employed):

$$\mathbf{e} = \mathbf{s}_p - \mathbf{s}_m \quad (7)$$

The time derivative of **e** is equal to:

$$\dot{\mathbf{e}} = \dot{\mathbf{s}}_p - \dot{\mathbf{s}}_m = \frac{\partial \mathbf{s}_p}{\partial \mathbf{r}} \frac{\partial \mathbf{r}}{\partial t} = \mathbf{L}_s \frac{\partial \mathbf{r}}{\partial t} \quad (8)$$

To make **e** decrease exponentially to 0, $\dot{\mathbf{e}} = -\lambda_2 \mathbf{e}$, we obtain the following control action:

$$\frac{\partial \mathbf{r}}{\partial t} = -\lambda_2 \mathbf{L}_s^{+} \mathbf{e} \quad (9)$$

where λ_2 is a positive control gain. Once the error is cancelled the extrinsic parameters will be obtained.

2. From $\mathbf{M}_O^{MC}$ and the mini-robot kinematics ($\mathbf{M}_{MC}^{RVC}$), the homogeneous transformation matrix between object O and the RVC can easily be obtained as $\mathbf{M}_O^{RVC} = \mathbf{M}_{MC}^{RVC}\ \mathbf{M}_O^{MC}$.

3. In order to perform this strategy, the 3D pose of the characteristic points with respect the frame O, $\mathbf{P}_u^O$, is known. Using this information and the matrix $\mathbf{M}_O^{RVC}$, the pose of the characteristic points with respect RVC are equal to $\mathbf{P}_u^{RVC} = \mathbf{M}_O^{RVC}\ \mathbf{P}_u^O$. Considering $\left(x_u^{RVC}, y_u^{RVC}, z_u^{RVC}\right)$ the coordinates of the previous pose, Equations (5) and (6), can be applied to obtain the value of the visual features in pixel coordinates relative to the image reference frame $\mathbf{s}_u$. These features will be the extracted features used at each iteration of the task.

4. As it is performed in classical image-based visual servoing, the desired features are extracted by using a learning stage in which the main robot is moved to the desired location. In this stage, the pose of the mini-robot is unknown. Therefore, when the main robot achieves the desired location, the pose of the mini-robot is unknown. Furthermore, in different experiments, the mini-robot can reach different locations for the same desired position of the main robot. To learn the desired features ($\mathbf{s}_{ud}$) the steps 1-4 must be performed but considering the main robot located at the desired pose.

4 EXPERIMENTAL RESULTS

In this section, different visual servoing experiments are described in order to show the correct behaviour of the strategy described in the paper. As it is previously indicated, in order to apply the image-based control a previous learning of the desired features employed to guide the main robot must be performed. To do so, first the main robot is located at the desired pose. At this moment, the mini-robot pose is unknown (the mini-robot can be located at any location). The desired features $\mathbf{s}_u^*$ are calculated from the visual features extracted by the mini-robot following the steps 1-4 described in Section 3.2.

4.1 Experiment 1

In this first experiment, four point features are extracted by the camera located at the mini-robot. These features are the corners of a square pattern of side 10 cm. The camera intrinsic parameters are (u_0, v_0) = (152, 118) px, and (f_u, f_v) = (388.9, 385.5) mm. This experiment consists of a positioning task in which the main robot desired location and the corresponding visual features $\mathbf{s}_u^*$ are represented in Figure 3. Figure 3.b represents the pose of the RVC (this pose coincides with the pose of the main robot end-effector). Furthermore, the mini-robot and main robot initial poses are shown in Figure 4 and Figure 5 respectively. These figures show the initial camera location and the extracted visual features from theirs poses.

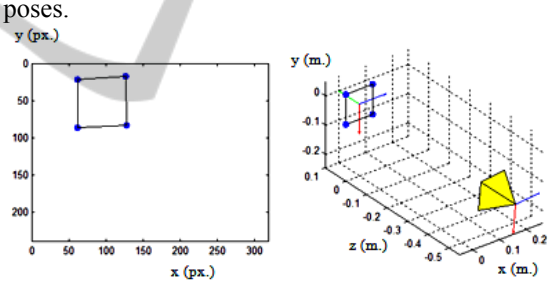

Figure 3: a) Desired visual features employed to guide the main robot using the RVC. b) Desired pose of the main robot (experiment 1).

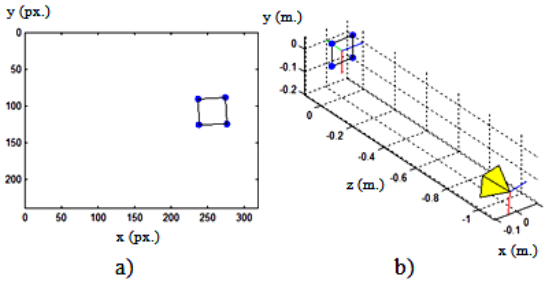

Figure 4: a) Initial visual features observed by the camera located at the mini-robot. b) Initial pose of the camera at the mini-robot (experiment 1).

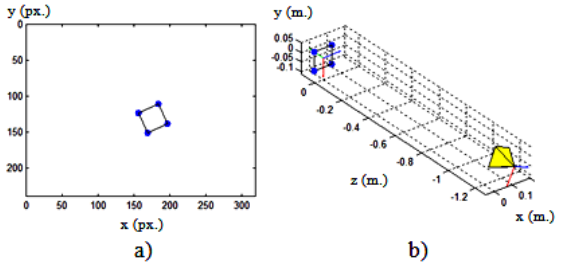

Figure 5: a) Initial visual features observed by the RVC. b) Initial pose of the RVC (experiment 1).

Using the proposed visual servoing approach, the trajectories presented in Figure 6 are obtained. In this figure, the camera at the end of the mini-robot is shown in yellow and the RVC trajectory in blue. It can be observed that the main robot achieves the desired pose. In order to observe clearly the precision during the positioning task, the image trajectory is represented in

Figure 7. This figure represents the evolution of the image features extracted by the RVC during the task. It can be seen that the final visual features are these ones indicated in Figure 3.

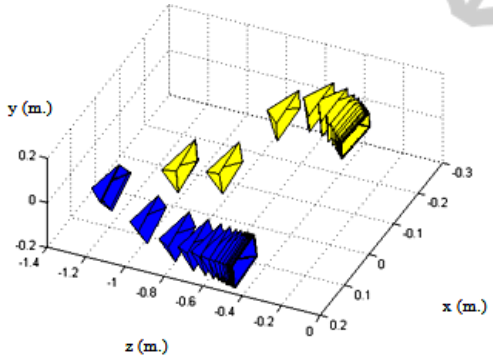

Figure 6: 3D trajectory during the task. In blue is represented the RVC trajectory and in yellow the mini-robot trajectory (experiment 1).

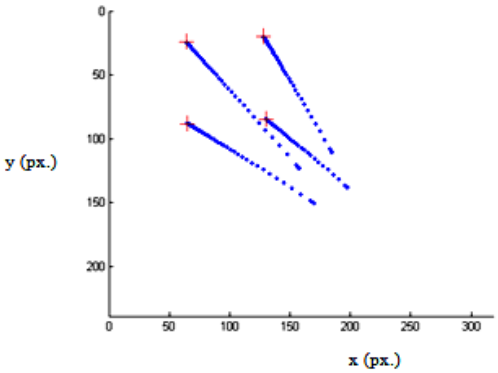

Figure 7: Image trajectory during the task (evolution of the image features observed by the RVC, experiment 1).

4.2 Experiment 2

This second experiment represents a position task in which a greater displacement is required. In this case, the features are the corners of a square pattern of side 25 cm. The camera intrinsic parameters considered in this experiment are $(u_0, v_0) = (256, 256)$ px, and $(f_u, f_v) = (1000, 1000)$ mm.

In this experiment, the desired main robot pose and the corresponding visual features $\mathbf{s}_u^*$ are represented in Figure 8. Furthermore, the mini-robot and main robot initial poses are shown in Figure 9 and Figure 10 respectively.

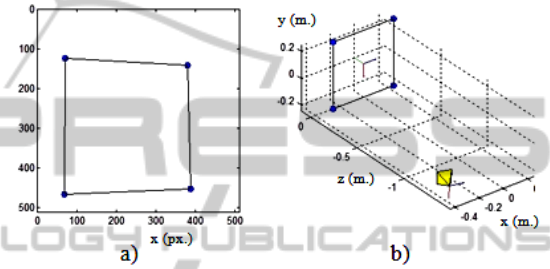

Figure 8: a) Desired visual features employed to guide the main robot using the RVC. b) Desired pose of the main robot (experiment 2).

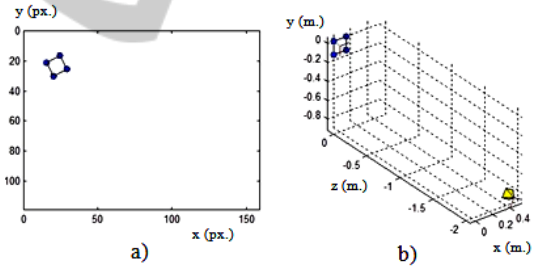

Figure 9: a) Initial visual features observed by the camera located at the mini-robot. b) Initial pose of the camera at the mini-robot (experiment 2).

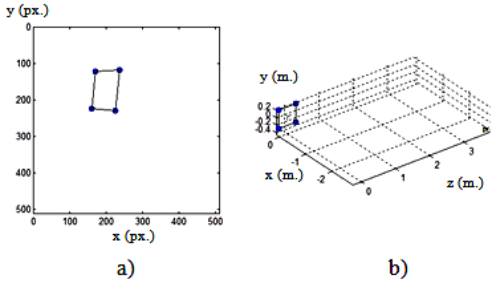

Figure 10: a) Initial visual features observed by the RVC. b) Initial pose of the RVC (experiment 2).

Using the proposed visual servoing approach the trajectories presented in Figure 11 are obtained. A

correct behaviour is also obtained. As shown in the previous experiment, the image trajectory is represented in Figure 12. This figure represents the evolution of the image features extracted by the RCV during the task. It can be observed that the final visual features converge towards the desired ones correctly.

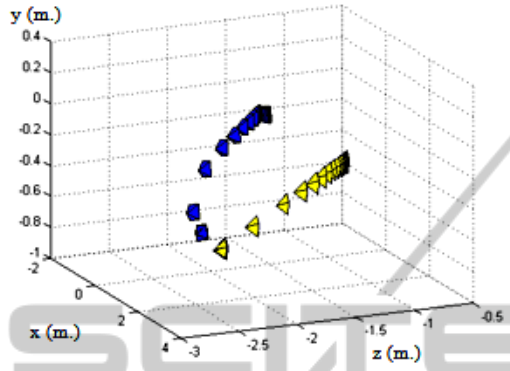

Figure 11: 3D trajectory during the task. In blue is represented the RVC trajectory and in yellow the mini-robot trajectory (experiment 2).

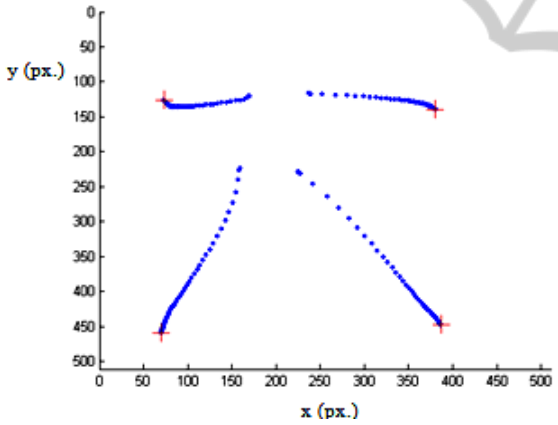

Figure 12: Image trajectory during the task (evolution of the image features observed by the RVC, experiment 2).

5 CONCLUSIONS

In order to improve the scene visibility in manipulation tasks a mini-robot has been attached at the end-effector of a Mitsubishi PA-10 manipulator. This mini-robot performs a path tracking task using visual servoing in order to decrease the occlusions in the scene. Through the visual information obtained by the camera located at the end-effector of the mini-robot, a method to obtain a virtual camera at the PA-10 end-effector has been proposed. This virtual camera provides the images employed by a visual servoing system to position the PA-10 with respect to the object to be manipulated. The experiments show the correct behaviour of the method proposed, where the images acquired by the real camera provide the necessary information to move both robots towards their goal position. Moreover, the proposed approach must be applied independently of the robot kinematic properties.

ACKNOWLEDGEMENTS

The work presented in this paper is supported by the Spanish Ministry of Education and Science (MEC) through the research project DPI2008-02647.

REFERENCES

Chaumette, F., Hutchinson, S., Visual servo control. I. Basic approaches. IEEE Robotics & Automation Magazine. Vol 13, Num 4, pp. 82-90. 2006.

Flandin, G., Chaumette, F., Marchand, E. Eye-in-hand/eye-to-hand cooperation for visual servoing. In *IEEE International Conference on Robotics and Automation*. Vol. 3, pp. 2741-2746, 2000.

Iwatani, Y., Watanabe, K., Hashimoto, K. Visual tracking with occlusion handling for visual servo control. In *IEEE International Conference on Robotics and Automation*, pp. 101-106, 2008.

Lippiello, V., Siciliano, B., Villani. L. Position-Based Visual Servoing in Industrial Multirobot Cells Using a Hybrid Camera Configuration. IEEE Transactions on Robotics. Vol. 23, Num. 1, pp. 73-86. 2007.

Muis, A., Ohnishi, K. Eye-to-hand approach on eye-in-hand configuration within real-time visual servoing. IEEE/ASME Transactions on Mechatronics. Vol. 10, Num. 4, pp. 404-410. 2005.

Pomares, J., Candelas, F., Torres, F., Corrales, J. A. García, G. J. Safe human-robot cooperation based on an adaptive time-independent image path tracker. Journal of Innovative Computing, Information and Control. Vol. 6. Num. 9. pp. 3819-3842. 2010.

Unal, H., Sen, U. y Mimaroglu, A., 2004 Dry sliding wear characteristics of some industrial polyme against steel counterface", Tribology International, vol. 37, pp. 727-732.